Green Process Synth 1 (2012): 109–127 © 2012 by Walter de Gruyter • Berlin • Boston. DOI 10.1515/greenps-2011-0510

Intensified demulsification and separation of thermal oxide reprocessing interfacial crud (THORP-IFC) simulants

Galip Akay[1,*], Turgay Pekdemir[1,2], Abdelmalik M. Shakorfow[1] and John Vickers[1,3]

[1] Process Intensification and Miniaturization Centre, School of Chemical Engineering and Advanced Materials, Newcastle University, Newcastle upon Tyne NE1 7RU, UK, e-mail: Galip.Akay@Newcastle.ac.uk
[2] ALSTOM (Switzerland) Ltd, Abt. TTFT, Zentralstrasse 40, Bld. 229, 5242 Birr, Switzerland
[3] British Nuclear Fuels Limited (BNFL), Sellafield, CA20 1PG, UK

* Corresponding author

Abstract

Reprocessing of spent nuclear fuel for the recovery of the fissionable materials (mainly uranium and plutonium), is performed by solvent extraction. Thermal oxide reprocessing (THORP) is the most widely used technique in which processing fluids gradually degrade and form stable emulsions that are referred to as interfacial crud (IFC). IFC is highly viscous and stable and its deposition in the nuclear reprocessing circuit results in blockages and plant shutdown for the recovery of IFC and cleaning of the lines. IFC is also encountered in other non-nuclear extraction processes such as crude oil production from oil wells due to the presence of naturally occurring surface active species in crude oil. In this study, we first investigated the synthesis of a non-radioactive IFC simulants and subsequently examined its demulsification behavior (separation into oil and aqueous components). It was concluded that the IFC is stabilized by surface active species, the removal of which results in the demulsification and subsequent phase separation and the prevention of the IFC re-formation. Demulsification was carried out using sulfonated, microporous, crossed-linked materials known as PolyHIPE Polymers (PHP). Demulsification characteristic of the hydrophilic PHP is unique compared with other demulsifiers, since the capture of surface active species is largely irreversible and hence, demulsified IFC does not reform upon mixing of the oil and aqueous phases. It is therefore possible to remove surface active species from the reaction circuit continuously.

Keywords: demulsification; interfacial crud; nuclear reprocessing; oil-water separation; polyHIPE polymer.

1. Introduction

1.1. Emulsions and demulsification

Emulsion break-up (demulsification) is an important process in numerous industries, for example, the oil industry, where the crude oil is separated from water. Crude oil-water emulsions are formed when water is used to displace oil and during pumping of the mixture of crude oil and water. Depending on the natural surface active species present in crude oil, the separation process can be very slow and expensive if the original oil-water mixture is in the form of fine emulsion stabilized by surface active species (such as resins and asphaltenes in the case of petroleum and various surface active agents, including particles, in other emulsions). However, the demulsification process can be accelerated by some external means such as applying an electric field and/or internal actions such as adding chemicals (referred to as emulsion breakers or demulsifiers). The combination of the demulsification method (using either demulsifiers or membrane based processes) with an electric field also yields intensification of demulsification and subsequent separation of oil and aqueous components [1–12].

If demulsification and separation of crude oil from water were to be achieved off-shore on drilling platforms, or even more importantly, if the emulsion formation is prevented in the first instance, pumping of large quantities of water (as the aqueous phase of the crude oil/water emulsion which can constitute up to 90% of extracted oil) can be prevented and the use of chemicals/solvents would not be required in the on-shore separation. This can only be achieved by permanent removal of surface active species from the oil phase. Therefore, the permanent removal of surface active species becomes part of the new process in operations where undesirable emulsification takes place, which then requires a demulsification stage [3, 5].

1.2. Emulsion formation during nuclear reprocessing

Unwanted emulsion formation occurs during the reprocessing of spent nuclear fuel in which the recovery of the fissionable materials (mainly uranium and plutonium) is performed by solvent extraction [13, 14]. The nature and structure of these emulsions encountered in nuclear reprocessing are significantly different compared with those encountered in crude oil-water emulsions. In solvent extraction during nuclear reprocessing, surface active species are formed, which in turn form multiple emulsions. The structures of these emulsions are similar to those encountered in some food emulsions

such as margarines and low fat spreads in the form of (oil-in-water)-in-oil (O/W/O). However, in nuclear reprocessing, the formation of such emulsions is highly undesirable due to their extreme stability, which results in fouling of processing equipment and in addition to the maintenance costs, this radioactive emulsion has to be recovered and stored until the radioactivity decays. Alternatively, it can be demulsified, and after the removal of surface active species, fissionable fractions can be returned for enrichment. As the formation of surface active species is unavoidable, the nuclear reprocessing plants can be modified with *in-situ* capture and removal of such emulsions, known as Chalk River unidentified deposit (CRUD) [13, 14]. Capture and recovery of radioactive CRUD will not only make the reprocessing more efficient, but will also reduce the volume of the radioactive waste.

In strict terms, nuclear electricity generation is neither renewable nor "green"; it is nevertheless seen as a possible pathway to combat global warming, at least in the short term. The thermal oxide reprocessing (THORP) technique, also known as the plutonium-uranium extraction (PUREX) process, is the most widely used in which the spent fuel is dissolved in 3 to 6 M nitric acid (HNO_3), referred to as the aqueous phase. The dissolved heavy metals are extracted by using an organic solvent, usually a 30% (by volume) tri-*n*-butylphosphate (TBP; extractant) in normal paraffin hydrocarbon (diluent), *n*-dodecane or odorless kerosene (OK; mainly dodecane with other alkanes C_nH_{2n+1}; $9 \leq n \leq 12$), referred to as the organic or solvent phase.

In the THORP, both the extractant and the diluent are gradually degraded to radiolysis products, including surface active materials, which then aid the formation and stabilization of emulsions. These emulsions can be identified when the extraction mixture is allowed to rest; the emulsions appear at the interface between the organic and aqueous phases. The emulsion is referred to as interfacial crud (IFC), which also appears to contain colloidal solids resulting from the corrosion of system materials [14]. They are thought to be either water-in-oil (W/O) or oil-in-water (O/W) types of emulsion. It is also likely that IFC is a multiple emulsion [(oil-in-water)-in-oil; O/W/O or (water-in-oil)-in-water; W/O/W]. One type (W/O or O/W) separates out immediately upon standing while the second type occupies the interface. Although the amount of the IFC formed is small, it nevertheless causes several problems in the extraction process, such as decreased mass transfer and fouling of the extraction and transport equipment. Although the chemistry of the radiation induced degradation of the extractant and diluent and formation of IFC have been widely investigated [14–21], the mechanism of formation and the structure of IFC have not been fully understood, because of its extremely complex and highly radioactive nature. For the effective operation of the PUREX process and the recovery of both the aqueous and organic phases from the IFC, it is thus essential to develop a process to prevent the formation of the IFC or to break down the IFC formed. One constraint is that this process must be suitable for being incorporated into the PUREX process, as well as robust enough to operate for long periods of time with minimum maintenance and replacement. These conditions, therefore, restrict the technique of demulsification and/or the disruption of emulsion formation.

1.3. Process intensification in demulsification

Simultaneous demulsification and separation of O/W and W/O emulsions can be achieved by contacting the emulsion with hydrophobic or hydrophilic surfaces, followed by the removal of the components of the emulsion from the demulsification zone. This process can be performed by using hollow fiber membranes or through the application of an electric field or the combination of different processes with an electric field [1–12]. The presence of the colloidal particles in IFC will have a stabilizing effect on the emulsion and therefore both the demulsification and the retention of the particles and/or surface active materials will be crucial in the demulsification of the IFC. It can be expected that, although the demulsification can be achieved temporarily by disturbing the thermodynamic conditions at the interface, unless the surface active species are removed from the oil/water binary system, these emulsions will reform if the oil/water mixture undergoes continuous deformation. Therefore, the removal of the degradation products or the surface active species should result in a permanent demulsification and separation.

The removal of surfactant structures in water using crossflow membrane filtration in the presence or absence of an electric field has been studied [22–25]. The surfactants were adsorbed within the pores of the membrane and formed highly stable lyotropic phases which acted as the secondary membrane controlling the permeate flux. Furthermore, surfactant based separations, including those based on membrane crossflow filtration, can also be intensified by the application of an electric field [5, 12, 25]. Surfactant capture and stabilization within micropores has been rationalized as a "confinement phenomenon" [26]. This phenomenon may be used for the selective removal of surface active species from water [22–25, 27] or applied to the intensification of several other processes [5]. For example, this phenomenon has already been applied to the demulsification of highly stable water-in-crude oil emulsions [12], using particles of hydrophilic microporous polymers known as PolyHIPE Polymers (PHPs) under static conditions [7], or under flow conditions in the absence or presence of an electric field [5, 12]. The other applications of the confinement phenomenon include tissue engineering [28, 29] and bioprocess intensification [30].

1.4. Novel demulsifiers for surfactant capture

The polymeric foams used as demulsifiers, or membranes in crossflow or dead-end filtration mode, are prepared through polymerization of a high internal phase emulsion (HIPE), in which the continuous phase contains the polymerizable components of the emulsion. These polymers can be produced either as particles, molded separation modules, or membranes; detailed relevant information is available elsewhere [3, 5, 24, 29, 31]. The resultant polymeric material is called PHP, reflecting its processing history [29, 31]. These polymers are hydrophobic, but they can be sulfonated to render them

hydrophilic, and can then be used as ion exchange media [31, 32]. Because of their highly open pore structures, the rate of ion exchange is very high compared with the conventional ion exchange resins [5, 32].

2. Experimental

This study can be divided into three main areas, namely: (1) preparation of a simulant (model) IFC, which should reflect all of the known properties of the THORP IFC as far as possible; (2) preparation and characterization of PHP as the demulsification material; (3) batch experiments for the demulsification and separation of IFC using various forms of PHP.

2.1. Preparation of model emulsion to simulate interfacial crud (IFC)

The model emulsion was prepared in a laboratory pilot plant scale experimental rig. The equipment consisted of a 40 l jacketed stainless steel reaction vessel fitted with a mechanic stirrer, a thermocouple and a constant temperature bath for water circulation through the jacket. The chemical materials used in the preparation of the simulant IFC were TBP, OK, nitric acid (HNO_3), palladium (Pd), sodium nitrite ($NaNO_2$) and double distilled water. Palladium powder was supplied by Goodfellows, Huntington, UK, while all other chemicals were supplied by Sigma-Aldrich, Gillingham, UK.

The non-radioactive model IFC production was as follows. A mixture of 10 l of 30% (by volume) TBP in OK and 10 l of 3 M HNO_3 solution containing a predetermined amount of transition metal (Pd) were taken in to the reactor. The Pd concentration varied up to 3 g/l in the initial aqueous phase. The temperature of the reactor was kept constant at a predetermined level throughout the reaction period of 144 h (6 days), while stirring it with the mechanical stirrer continuously. The effect of temperature was investigated in the range of 50–80°C. The effect of the $NaNO_2$ addition, which was to simulate the effect of the radiation induced oxidative degradation, was studied in the range up to 40 g/day. At the end of each 24 h of the operation, the stirring of the reactor content was stopped for 1 h. This allowed the separations of the aqueous and organic phases prior to sampling them for analysis, and $NaNO_2$ was added after sampling. After a 6-day (144 h) operation period, the reactor content was allowed to cool down to room temperature and then emptied into storage vessels for settling. Three phases formed in the vessels after the settling completed: (1) the aqueous phase at the bottom; (2) the IFC phase in the middle (if available) and (3) the organic phase at the top. These three phases were separated from each other by using a separation funnel. The IFC phase was collected in dark colored Winchester bottles for analysis, as well as for the batch mode demulsification tests.

Samples of the aqueous phase, organic phase and IFC were analyzed for concentrations of the following species: total organic carbon (TOC), carboxyl group (-COOH), Pd, and DBP. Emulsion conductivity was recorded and the structure was examined using transmission electron microscopy (TEM). Solids obtained from dried emulsion samples or solids recovered by the demulsifier PHP were analyzed using scanning electron microscopy (SEM) equipped with an energy dispersive analytical X-ray (EDAX). X-ray diffraction (XRD) was used for Pd analysis. The concentrations of various elements (H, C, N, P, Pd) in the emulsions or within the pores of the demulsifier were determined using atomic absorption spectroscopy (AA) and inductively coupled plasma spectroscopy (ICP). The degree of the degradation can be inferred from the variation of concentrations of -COOH, DBP, Pd in the aqueous and organic phases and TOC concentration in the aqueous phase.

2.2. Preparation of PHP

The preparation of HIPEs and their use in the production of PHP materials have been described previously [22–24, 29]. The void volume of the polymer can be as high as 98%, while the pore size can be controlled accurately from hundreds of μm to a μm [29, 31]. The PHP can be elastic or rigid, depending on the type and proportion of monomers used in the oil phase. They can be made hydrophobic or hydrophilic. In this work, the continuous oil phase of the HIPE for a rigid PHP was made from a mixture of styrene with the crosslinking agent divinyl benzene (DVB) and a W/O emulsifier (surfactant), Span 80. A typical oil phase composition (by volume) was styrene; 78%, DVB; 8%, and Span 80; 14%. The dispersed aqueous phase comprised a solution of a polymerization initiator, potassium persulfate (0.5% by mass), in double distilled water.

A sufficient amount of aqueous phase was dosed into the stirred oil phase until an aqueous to oil phase ratio 90:10 (by volume) was achieved over a period of about 10 min. The HIPE was stirred for a further 20 min before it was taken into the molds. They were polymerized in an oven at 60°C overnight, dried, and chopped into about 1 cm cube pieces. The PHP pieces were washed free of surfactant with isopropyl alcohol (IPA) and water and re-dried.

Sulfonated PHP (S-PHP) becomes acidic as $-SO_3^-H^+$ groups are attached to the benzene rings of the crosslinked polystyrene chain. The method of sulfonation is available elsewhere [24, 29]. If the degree of the sulfonation is expressed as the percentage of available benzene rings in the polymer structure which can attain $-SO_3^-H^+$ groups, it can be quantified by a titrimetric analysis. Hydrophilicity of the PHP can thus be tuned to the desired level by adjusting the degree of the sulfonation.

The PHP sulfonation is performed by contacting the PHP with sulfuric acid. Details of the sulfonation have been explained elsewhere [24, 29]. In the present work, PHP pieces were soaked in 98% (by mass) acid with a reaction temperature varying between 20 and 90°C and varying periods of time for various degree of the sulfonation. After being washed free of excess acid and dried, the degrees of sulfonation were determined by using titrimetric analysis. Alkali salts of the PHP can be prepared by contacting it with aqueous alkali solutions following the sulfonation. This causes an exchange between protons in $-SO_3^-H^+$ groups and positively charged ionic species of the alkalis. The sodium salt of sulfonated PHP (i.e., neutralized PHP [S-PHP-Na]), was prepared by

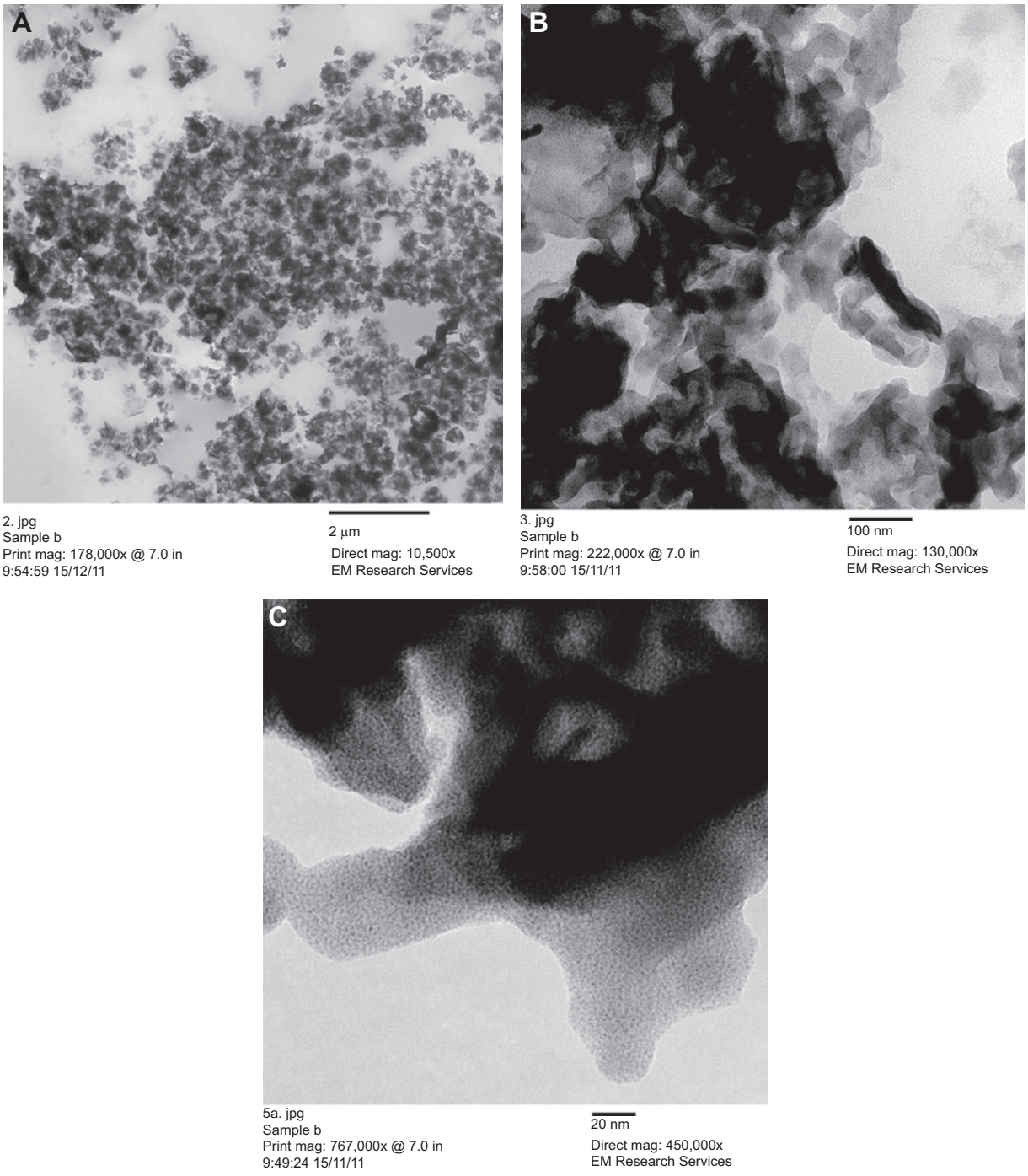

Figure 1 Transmission electron microscopy study of IFC showing the presence of multiple emulsions. Dark areas represent palladium rich regions mainly in the aqueous phase. IFC production conditions: reaction temperature T=60°C when: [Pd]=1 g/l; $NaNO_2$ addition rate= 10 g/day. (A) Scale bar=2000 nm, (B) scale bar=100 nm, (C) scale bar=20 nm. Unless stated otherwise, IFC used in the demulsification experiments were produced under the same production conditions.

soaking the S-PHP samples in 2 M sodium hydroxide. After neutralization, S-PHP-Na samples were washed in water to remove excess NaOH. The PHP pieces were chopped into small particles by using a domestic food processor and were finally sieved into the desired size fraction ready to be used in the demulsification tests.

2.3. Demulsification of IFC

In this study, the IFC was demulsified in a batch mode operation. The batch mode demulsification was performed in measuring cylinders of 50 ml capacity. A certain volume of the model crud samples was taken from a well shaken stock

bottle into the cylinder, which will be referred as tube hereafter, and allowed to settle down overnight. The volumes of the aqueous phase (if present), emulsion (crud), and organic phase (if present) were recorded prior to shaking the content with a vortex generator for 2 min. These volumes were taken as the initial phase volumes. A predetermined mass of PHP was then added into the tube and shaken for a further 2 min. Following the final shaking, the volumes of the three phases were recorded at certain intervals over a time period, until the separation curve reached a plateau. These volumes were taken as the final phase volumes. The initial and the final values were used in the calculation of the demulsification capacity, D, defined as:

$$D=\frac{\left[V_{aq}\right]_l-\left[V_{aq}\right]_i}{\left[M_{PHP}\right]} \quad (1)$$

where V_{aq} = the volume of the aqueous phase, M_{PHP} = the mass of the PHP particles. Indices i and l denote initial and final, respectively. The reason for using the volume of the aqueous phase in the demulsification capacity is that it is easier to determine more accurately than those of the IFC phase, which most of the time contains the PHP particles, and the organic phase.

3. Results

3.1. Preparation of model interfacial crud (IFC)

Model IFC emulsions (simulants) were made for varying reaction temperature, and daily sodium nitrite addition at three different Pd concentrations. The effect of each of these parameters was investigated as a function of processing time. Samples of aqueous and organic phases of 90 ml (three samples for each phase) were collected every 24 h for a period of total 144 h of continuous operation.

Conductivity measurements indicated that the simulants were either W/O or O/W/O type emulsions, as they displayed very low conductivities (up to 5.2 µS/cm). The structure of the IFC was determined by TEM (Figure 1A–C) at different magnifications. Here, the continuous oil phase is light colored, while the aqueous phase, which contains most of the Pd is dark colored. The inner oil phase is surrounded by the aqueous phase, thus forming an O/W/O emulsion. However, in places, the aqueous phase is also dispersed in the oil phase consistent with W/O emulsion structure.

The simulants were analyzed using SEM fitted with an EDAX facility, as well as other methods of chemical analysis. IFC samples were placed on the SEM sample holders and dried for SEM/EDAX analysis. The micrographs indicated that the IFC solids were in the form of sharp edged disk-shape like particles. These particles remained in the bulk either as individuals and/or formed agglomerates. The predominant X-ray spectra showed the presence of a large amount of Pd in the IFC solids. Some of the separated IFC solid samples were washed with ethanol and dichloromethane, followed by hexane to remove any TBP and OK residue followed by drying. These washed solids were analyzed by SEM/EDAX as well as by chemical methods for their H, C, N, P and Pd contents. Some typical SEM micrographs are given in Figure 2A–C. Figure 2A represents as-recovered IFC while Figure 2B and C represent the samples which were washed with ethanol and dichloromethane/hexane, respectively. Chemical analysis results for these same samples are given in Table 1. The chemical analysis confirmed the findings from EDAX spectrums. Powder X-ray diffraction of Pd used in the simulant crud production was compared in Figure 3 (A) with those of: (B) membrane separated crud solids; (C) centrifuge separated crud solids washed with ethanol; and (D) centrifuge separated and washed with dichloromethane followed with hexane. As seen from these figures, the solids recovered from

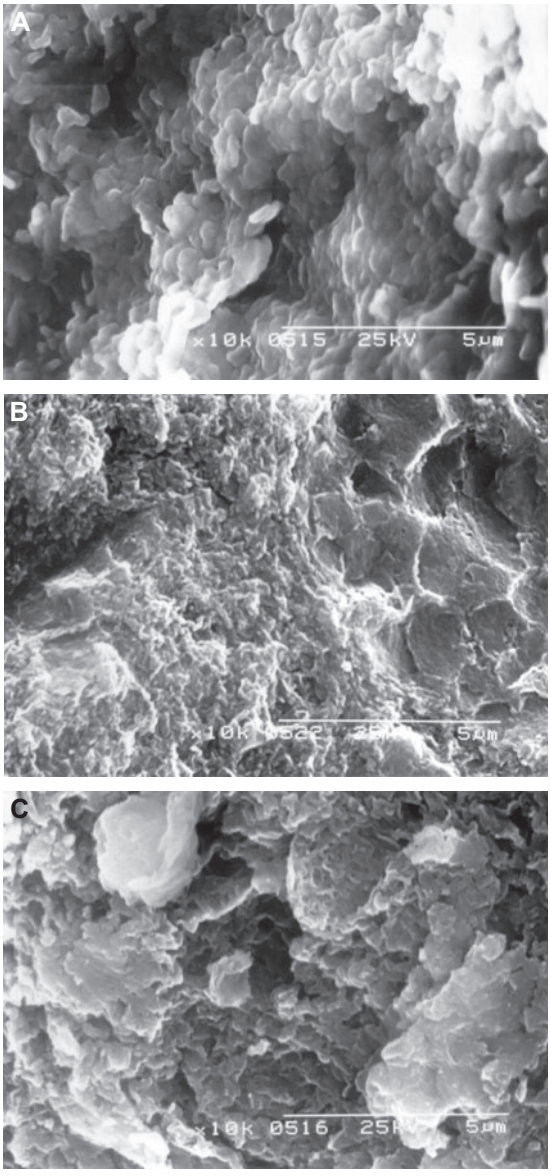

Figure 2 SEM micrographs of typical crud solids: (A) membrane separated; (B) ethanol washed; and (C) washed with dichloromethane followed by hexane. Scale bar=5 µm.

Table 1 Chemical analysis of the solids of a typical IFC.

Element	Concentration (%)					
	Original crud			Remaining crud after demulsification by PHP		
	MSOC	DCMWOC	EWOC	WWRC	DCMWOC	EWRC
Pd	19.33	35.66	37.17	18.25	22.11	21.58
P	0.58	0.07	0.10	0.62	0.38	0.38
C	39.86	15.72	20.10	60.28	27.78	30.31
H	6.20	0.59	1.34	5.05	1.66	1.96
N	5.82	9.44	10.79	4.10	6.69	6.06
Total	71.79	61.48	69.50	88.30	58.62	60.29
Others	28.21	38.52	30.50	11.70	41.38	39.71

MSOC, membrane separated original crud; DCMWOC, dicholoromethane washed original crud; EWOC, ethanol washed original crud; WWRC, water washed remaining crud; DCMWRC, dicholoromethane washed remaining crud; EWRC, ethanol washed remaining crud.

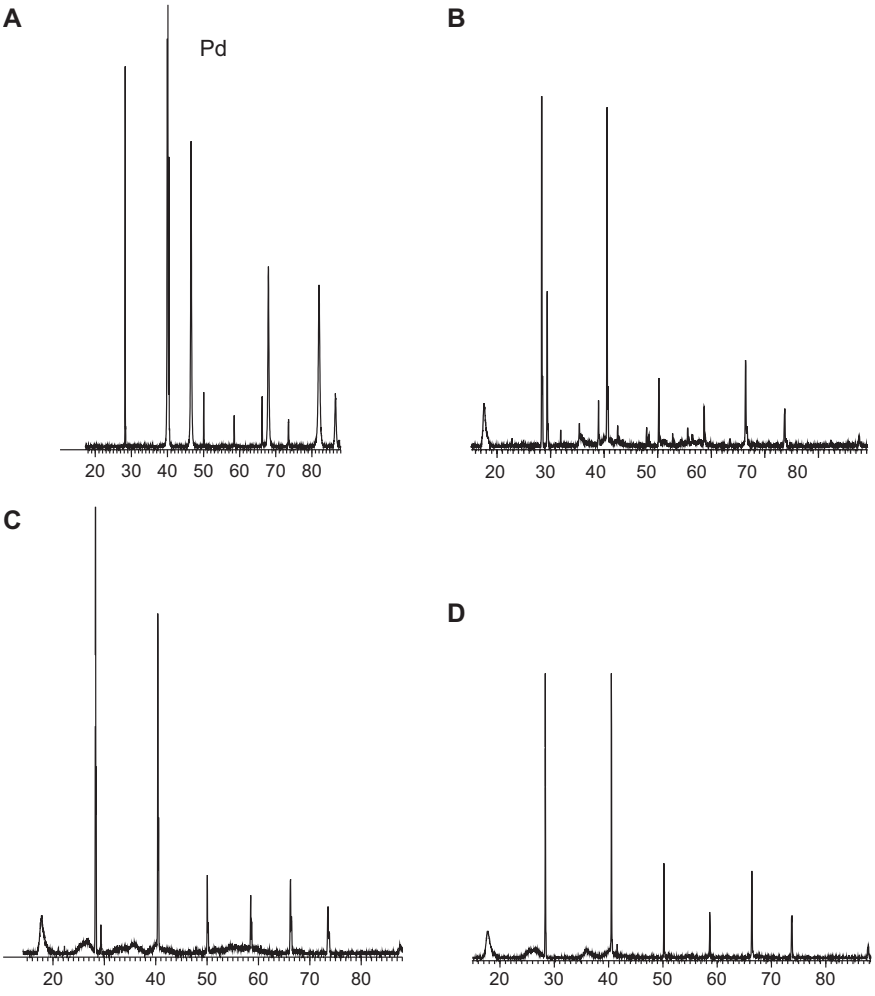

Figure 3 Comparison of powder X-ray diffractogram of: (A) palladium (Pd) used in the simulant crud production with those of; (B) membrane separated crud solids; (C) centrifuge separated crud solids washed with ethanol; and (D) centrifuge separated crud solids washed with dichloromethane followed with hexane.

the IFC contained, in addition to originally added Pd, other solids formed due to the degradation process as evidenced by the spectrums of the samples washed by the solvents (B–D) approaching to that of the original Pd.

3.1.1. Interfacial crud (IFC) yield The yield of IFC at the end of 144 h of reaction at a constant Pd concentration of 1 g/l was depended on $NaNO_2$ addition rate and, more significantly, on the reaction temperature. Figure 4A and B illustrate the

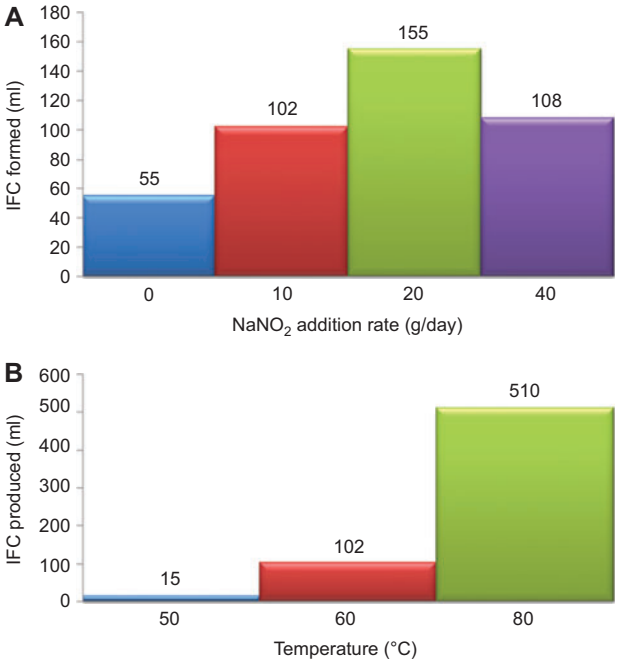

Figure 4 IFC yield as a function of (A) the $NaNO_2$ addition rate (reaction temperature=60°C) and (B) temperature ($NaNO_2$ addition rate=10 g/day) after 144 h of reaction at constant palladium concentration of 1 g/l.

IFC yield as a function of these two process variables. It is clear that temperature had the largest effect on the yield.

3.1.2. Effect of sodium nitrite addition The effect of daily sodium nitrite addition was studied in a range up to 40 g/day at a constant Pd concentration of 1 g/l. The results are shown in Figures 5 and 6. The concentration of $NaNO_2$ did not significantly influence the quantity of IFC, when it exceeded 10 g/day. The effects of varying the $NaNO_2$ concentration as a function of the operation time on the concentrations of -COOH, DBP, Pd, and TOC in the aqueous phase, are shown in Figure 5. Concentrations of -COOH and TOC increased, Pd concentration decreased and DBP concentration did not significantly change with time as a result of the degradation of the organic phase as well as Pd partitioning between the aqueous and solvent phase. In general, the concentrations of -COOH and TOC increased with increasing $NaNO_2$ concentration, whereas DBP and Pd concentrations were not significantly affected. This indicates that the solvent phase degrades into carboxylic acids, as well as other water soluble components, with time and that the degree of the degradation increases with increasing amount of $NaNO_2$. Figure 6 shows the variations of the concentrations of -COOH, DBP, and Pd in the organic phase as a function of time and $NaNO_2$ concentration. Concentrations of -COOH, TOC and Pd increased with time. The effect of $NaNO_2$ concentration on the concentrations of DBP and Pd, in the organic phase, was

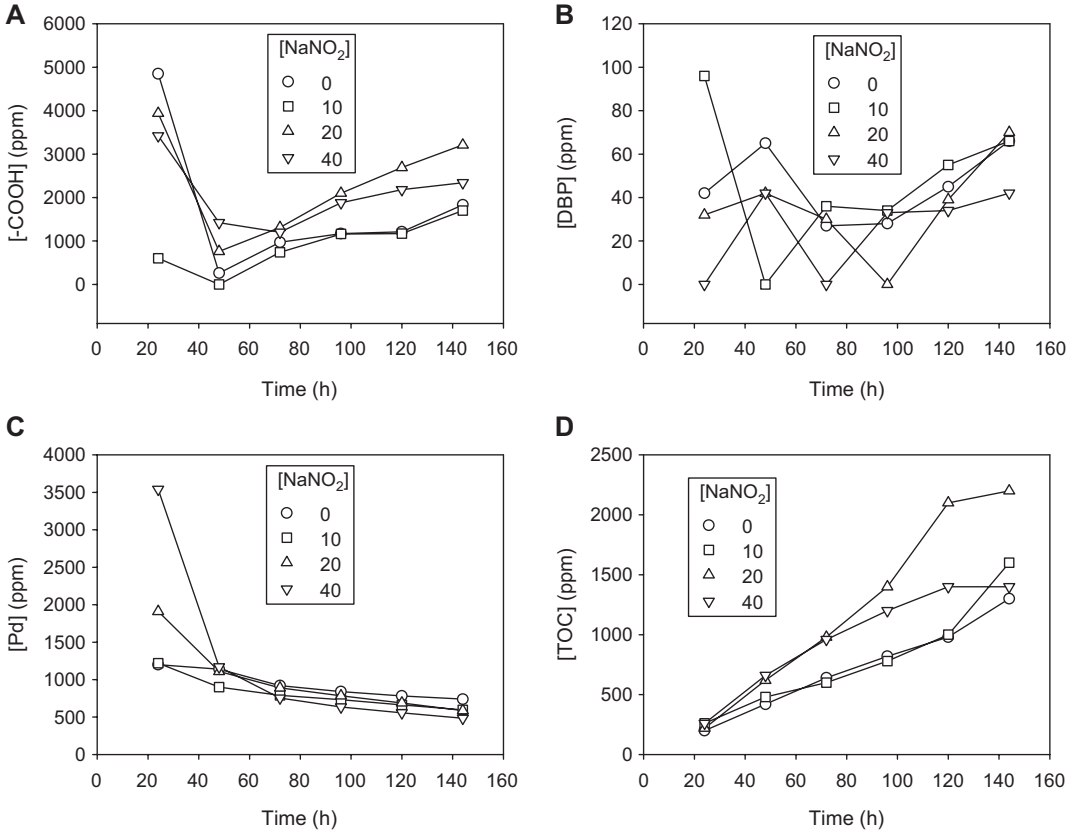

Figure 5 Effect of the daily sodium nitrite addition on the variation of: (A) [-COOH]; (B) [DBP]; (C) [Pd]; and (D) [TOC] in the aqueous phase as function of the operation time.

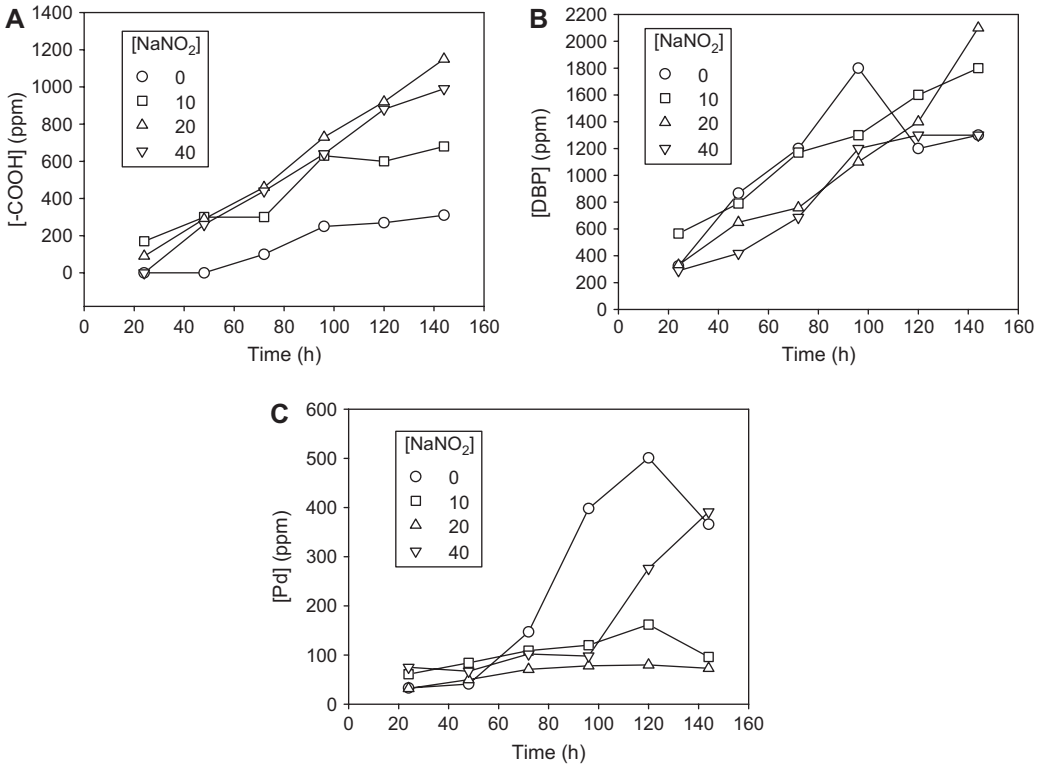

Figure 6 Effect of the daily sodium nitrite addition on the variation of: (A) [-COOH]; (B) [DBP]; and (C) [Pd] in the solvent phase as function of the operation time.

different from than that in the aqueous phase. The data for the variation of DBP concentration with $NaNO_2$ concentration indicates no clear trend as it is time dependent. It was reported [19–21] that under severe oxidation conditions, the degradation of TBP can lead to the formation of DBP as well as monobutyl phosphate (MBP), which would make any conclusive trend difficult without further chemical analysis for MBP. The variation of Pd concentration with $NaNO_2$ concentration, on the other hand, shows both an increasing and a decreasing trend, especially after about 60 h of operation. This may indicate that Pd in the organic phase is bound by the degradation products, in the form of solid organo-metallic compounds, and accumulates in the IFC phase. This was supported by the increasing volume of IFC with $NaNO_2$ concentration (Figure 4). As shown in Figure 5C, for $NaNO_2$=20 g/day, the Pd concentration in the organic phase was the smallest, but the volume of the IFC was the largest.

3.1.3. Effect of reaction temperature The effect of the reaction temperature, T, was studied in the range of 50–80°C. The results are shown in Figures 7 and 8. It appeared that temperature was the most effective parameter in the formation of IFC. Results show that increases in the temperature caused a significant increase in the volume of IFC (Figure 4). The most significant effect on the variation of the degradation indicator parameters (-COOH, DBP, Pd, and TOC concentrations in the aqueous, and -COOH, DBP, and Pd concentrations in the organic phase) was a temperature of >60°C. It is seen from Figure 7 that -COOH and TOC concentrations showed a similar trend at temperatures ≤60°C; they did not change significantly with time but increased slightly with increasing temperature. When the temperature was raised to 80°C, they increased dramatically with both time and temperature, indicating a high-level of degradation. In the case of DBP concentration, at temperatures ≤60°C, no DBP was detected in the aqueous phase, but at 80°C, it firstly decreased from 100 ppm to 0 ppm, following which it increased gradually to 60 ppm. From this, and the variation of Pd concentration with time and temperature (Figure 7C), it may be inferred that at 50 and 60°C, no DBP is produced, and therefore Pd is not consumed by the formation of an insoluble DBP-Pd complex. Thus, at 50 and 60°C, the concentration of Pd remains high in the aqueous phase and slightly decreases with time after the initial rapid decay. This slight decrease (at a long reaction time) may be explained by Pd partitioning between the aqueous and organic phases. However, at 80°C, both Pd and DBP in the aqueous phase were reduced to almost to zero very quickly, by the complex formation between Pd and DBP. Once all the available Pd was consumed, the concentration of DBP generated by the degradation remained in the solution and its level thus increased with time. The effect of the temperature on the degradation indicators in the organic phase is shown in Figure 8. Variation of -COOH concentration with temperature as a function of time, was almost identical to that in the aqueous phase: at 50 and 60°C, there was no significant change with time and an increasing trend with increasing

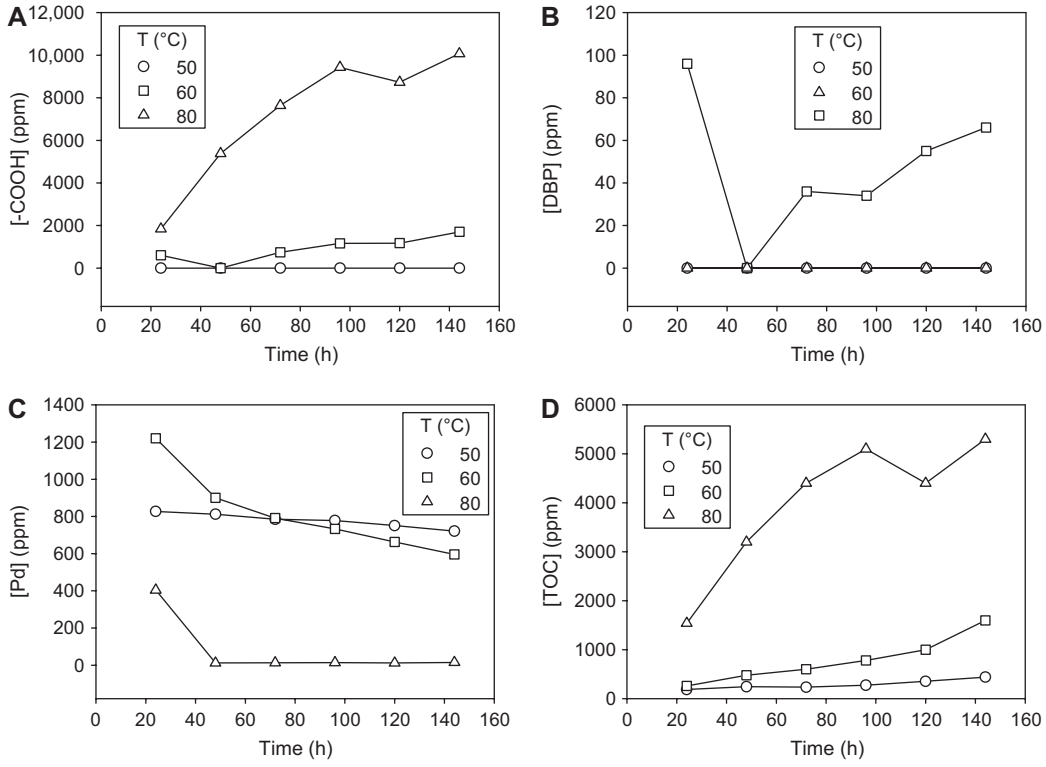

Figure 7 Effect of reaction temperature on the variation of: (A) [-COOH]; (B) [DBP]; (C) [Pd]; and (D) [TOC] in the aqueous phase as function of the operation time.

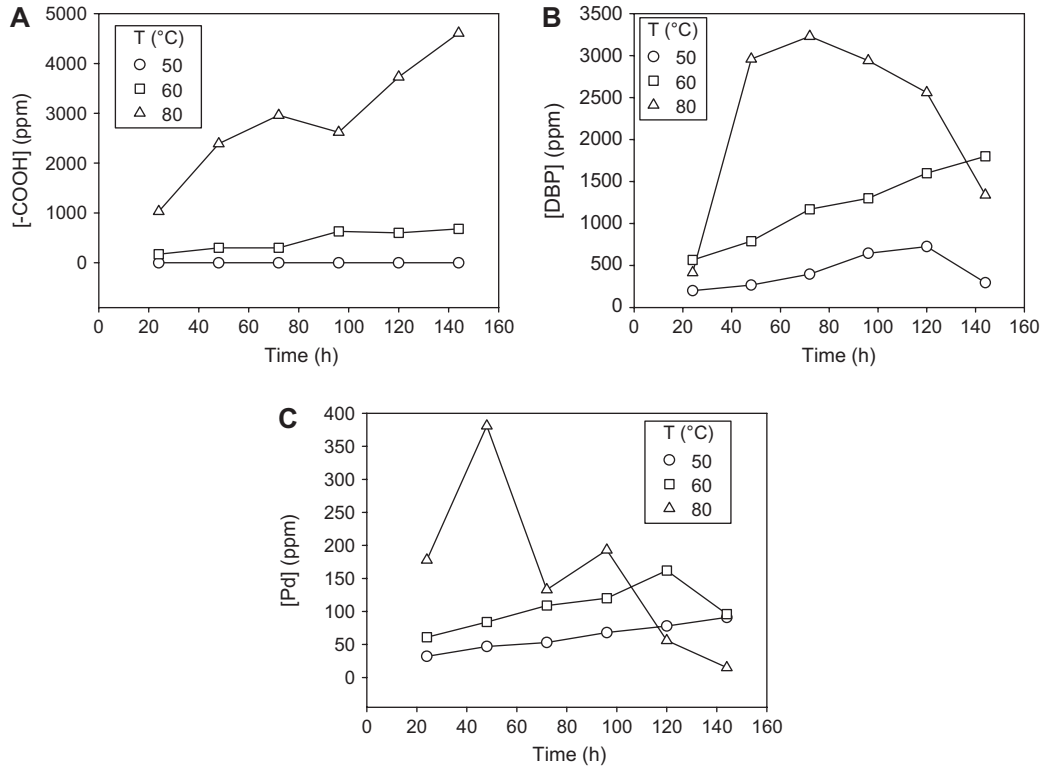

Figure 8 Effect of reaction temperature on the variation of: (A) [-COOH]; (B) [DBP]; and (C) [Pd] in the solvent phase as function of the operation time.

temperature. Variations of DBP and Pd concentrations with temperature, as a function of time, indicated that at 50 and 60°C, Pd and DBP may not be forming a water insoluble complex, as the concentration of Pd and DBP increased with time. This was supported by the volumes of IFC produced for these conditions (Figure 4). At 80°C, after about 40 h, both DBP and Pd concentrations decreased with time. This, and the volume of the IFC produced, indicate that DBP and Pd formed an insoluble complex and are placed in IFC. The formation of DBP and Pd complex was greatly influenced by temperature.

3.2. PHP and S-PHP production

Both rigid and elastic PHPs were prepared and a typical micrograph for a rigid PHP is given in Figure 9. This figure shows the cellular structure of the PHP, with the main cells interconnected by the smaller windows in the cell walls. S-PHPs have been prepared with varying degrees of sulfonation ranging from 10 to 96%. Figure 10 shows a micrograph of a typical S-PHP. It is seen that during the sulfonation, the PHP structure is etched by the concentrated sulfuric acid. This leads to the enlargement of the existing pores and formation of new smaller pores within the cell walls.

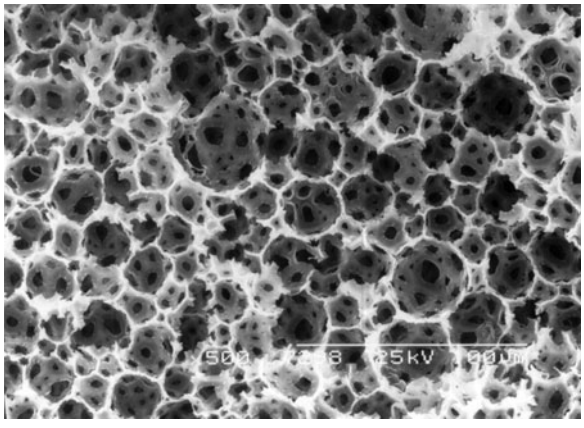

Figure 9 SEM micrograph of hydrophobic rigid PolyHIPE Polymer, PHP, before sulphonation. Scale bar=100 µm.

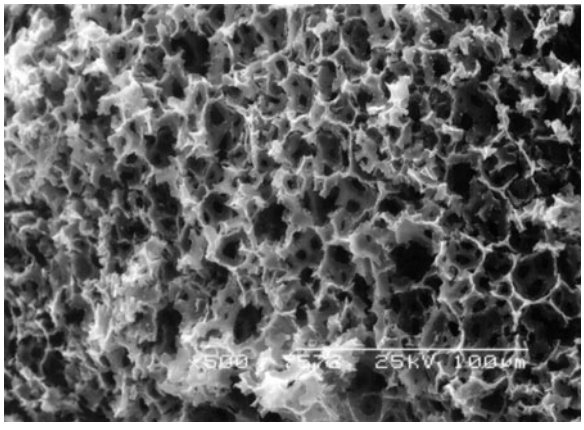

Figure 10 SEM micrograph of a sulphonated PolyHIPE Polymer, S-PHP (degree of sulphonation=70%). Scale bar=100 µm.

3.3. Demulsification of IFC

The demulsification experiments were carried out using IFC obtained under following conditions: Pd=1 g/l; $NaNO_2$ addition rate=10 g/day; T=60°C; total reaction time=144 h (6 days). The size range of the PHP particles used in the experiments was 1000 µm to 250 µm (see Table 2). The amount of PHP particles used was denoted by M_{PHP} and the volume of IFC by V_T. Following the mixing of PHP particles with IFC within the measuring cylinders, they were allowed to separate for 2 days and subsequently the volume of each separated layer recorded. After separation, it was observed that some PHP remained in the bottom layer while others were present in the middle layer.

The effect of PHP loading on the separation efficiency is diagrammatically shown in Figure 11, which indicates that if the PHP mass/IFC volume ratio (M_{PHP}/V_T) was increased above ~0.008 g/ml, hydrophilic PHP retained all of the IFC. The most efficient separation occurred at low values of PHP as shown in Figure 11. The results are summarized as follows:

- For $0.034 \leq M_{PHP}/V_T \leq 0.15$ (g/ml) rigid hydrophilic PHP adsorbed everything; no separation occurred.
- For $0.008 \leq M_{PHP}/V_T < 0.034$ (g/ml) no separation occurred; some free organic phase remained at the top.
- For $M_{PHP}/V_T < 0.008$ (g/ml) separation occurred; the separation got better for the smaller ratios.
- For $M_{PHP}/V_T = 0.001$ (g/ml) significant separation occurred; it became better with decreasing M_{PHP}/V_T.

The sediments in the aqueous phase, remaining IFC, and PHP particles positioned in the IFC phase were analyzed using SEM/EDAX.

Typical micrographs and an EDAX spectrum of the sediments are shown in Figures 12 and 13, respectively. These

Table 2 Summary of the sulphonation test.

Particle size (mm)	Temperature (°C)	Time (h)	Degree of sulphonation (%)
-1+0.25	40	2	10
-1+0.25	40	4	10
-1+0.25	40	23	10
-3*+1	40	4	19
5*	95	24	96
5*	95	1	89
5*	95	0.5	80
10*	75 and 95	3 at 75°C and 8 at 95°C	92
20*	95	16	92
20*	Room	18	12
20*	95	6	86
20*	95	3.5	70

*Approximate.

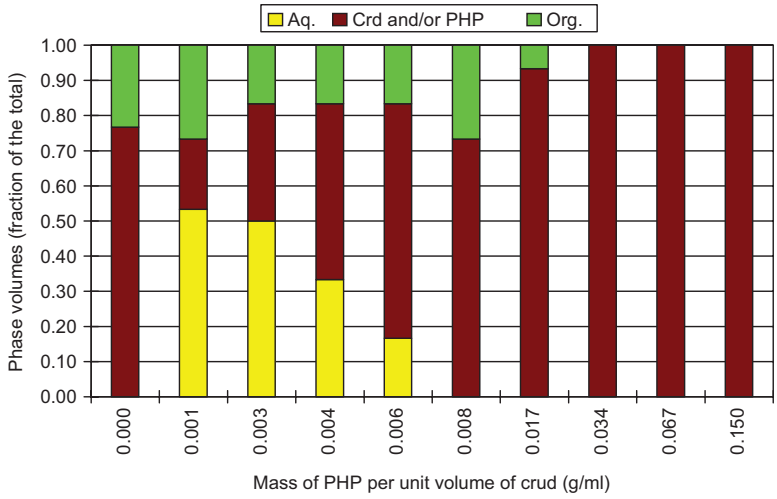

Figure 11 Performance of the sulfonated (hydrophilic) rigid PHP in the demulsification of IFC.

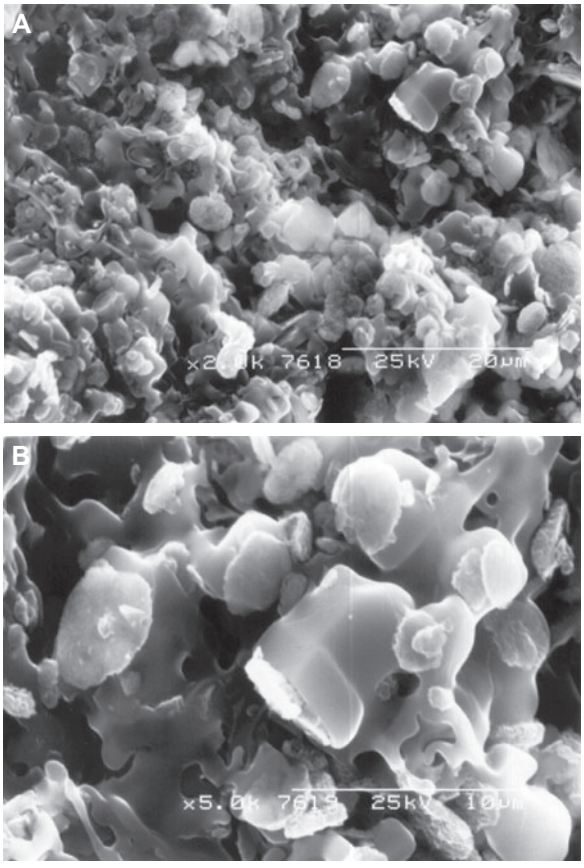

Figure 12 SEM micrographs of the sediments formed in the aqueous phase during the demulsification of crud by hydrophilic PHP. Magnification: (A) scale bar=20 μm, (B) scale bar=10 μm.

micrographs show that small particulate materials were trapped in the cellular structure of the PHP, whereas the larger ones accumulated on the surface. These large particulate materials may be: (1) the IFC particles adsorbed by PHP and sedimented with PHP, (2) and/or the IFC particles which are not adsorbed by PHP but are the sediment when PHP demulsifies the IFC resulting in the formation of the aqueous phase. Figure 13A is the EDAX spectrum of the total area shown by a micrograph in Figure 12A, while Figure 13B is the EDAX spectrum of a single crud particle trapped in the cell. These spectrums indicate the presence of palladium in the sediments.

Figure 14 shows typical micrographs of the PHP particles which remained in the IFC. These PHP particles had very little porosity left, as a result of which, they were unable to trap any more IFC solids. Being lighter than the aqueous phase, they were positioned in the remaining IFC phase after the demulsification.

Some separate samples of remaining IFC solids were washed with water, ethanol, and dichloromethane followed by hexane, to remove any TBP and OK residues, which might have remained on the solids. These washed remaining solids were analyzed by SEM/EDAX, as well as by chemical methods for their H, C, N, P and Pd contents. Some typical micrographs and X-ray spectra are given in Figures 15A and 16A for the samples washed with water, Figures 15B and 16B for the samples washed with ethanol and Figures 15C and 16C for the samples washed with dichloromethane and hexane. Chemical analysis results for these same samples are given in Table 1. As for the original crud, the micrographs indicated that the remaining crud solids also are in the form of sharp edged disk shape like particles. These particles again remained in the bulk either as individuals and/or they formed aggregates. The EDAX spectrum (shown in Figure 16) of the total area of the micrographs in Figure 15, indicates the presence of Pd in the remaining IFC.

3.3.1. Re-demulsification Some detailed demulsification tests were performed to investigate the demulsification of the remaining crud from the first demulsification test, by using both PHP and S-PHP-Na and also a combination of the two. In these tests, both types of crud, as well as ratios

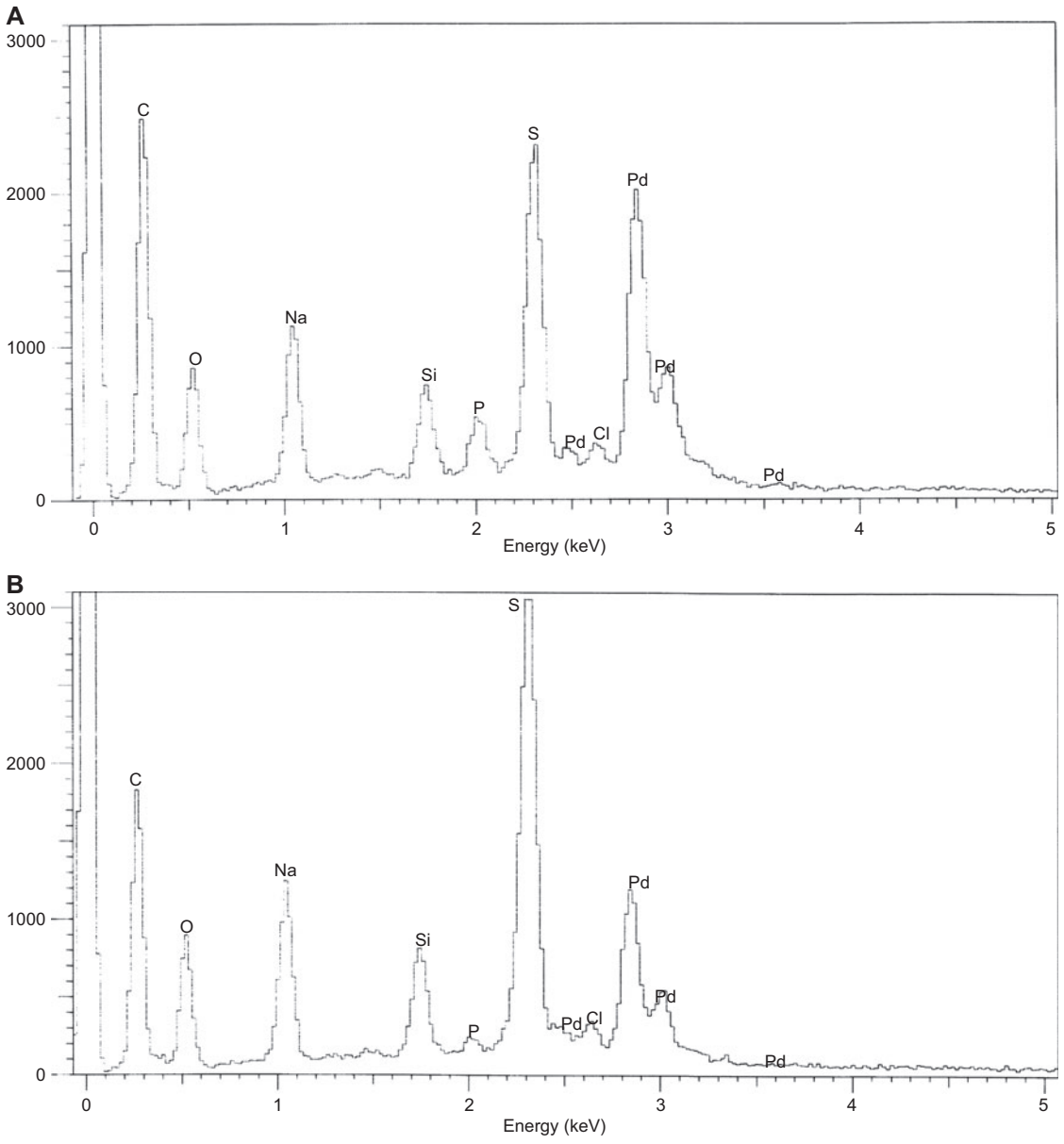

Figure 13 (A) EDAX spectrum of the sediments formed in the aqueous phase during the demulsification of crud by S-PHP-Na (total area shown in Figure 12A); (B) EDAX spectrum of the sediments formed in the aqueous phase during the demulsification of crud by S-PHP-Na (single particle in Figure 12B).

of PHP mass/crud volume changed. The PHP did not cause any further demulsification and PHP itself did not undergo any changes. The S-PHP-Na, by contrast, seemed to be absorbing the remaining IFC without causing any further phase separation. In contrast to the first demulsification, the colors of the S-PHP-Na particles changed into that of the IFC, becoming dark brownish-black. These S-PHP-Na particles were analyzed using SEM/EDAX. Figure 17 shows typical micrographs of the S-PHP-Na particles. The cell walls and pores of these S-PHP-Na particles were heavily plastered by very fine IFC solids, which appeared to be smaller than those absorbed initially. Furthermore, these particles were more rounded, probably indicating the presence of amorphous organics. The results indicate that the PHP is only capable of partially demulsifying IFC, by removing only certain agents stabilizing the IFC. Other means may have to be developed for the demulsification of the remaining IFC following the first partial demulsification by the S-PHP Na.

Some very fine particles from the IFC remained on the top of the PHP layer in the organic phase after re-demulsification. These fine particles were easily dispersed into the solvent phase with slight movement of the tubes. They were also analyzed using SEM/EDAX and typical micrographs and an EDAX spectrum are shown in Figures 18 and 19, respectively. Micrographs show that the disk like shape of the original IFC particles was not observed here, and that the fine IFC particles agglomerated into round edged larger particles. Figure 19A shows enhanced phosphorous peak with respect to that of Pd,

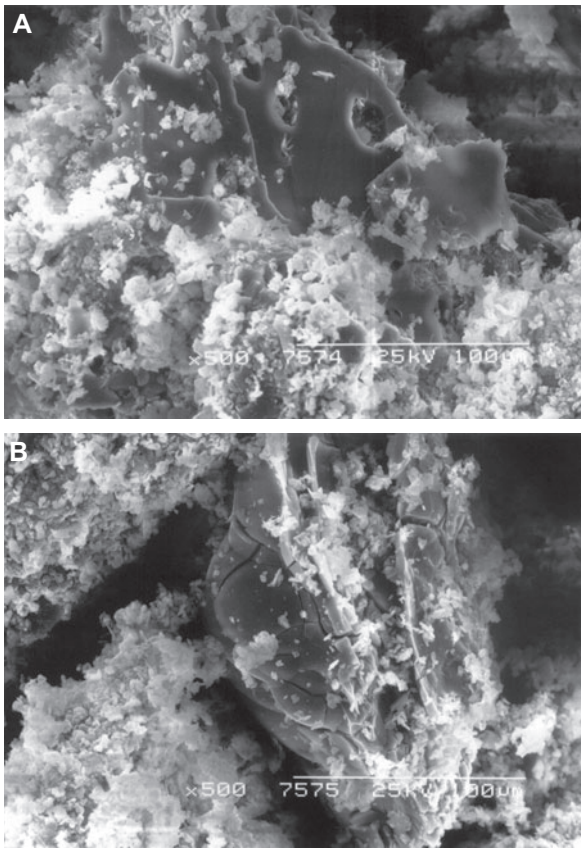

Figure 14 SEM micrographs of the S-PHP-Na particles remaining in the crud phase after the first demulsification. Scale bar=100 μm: (A) area-1, (B) area-2.

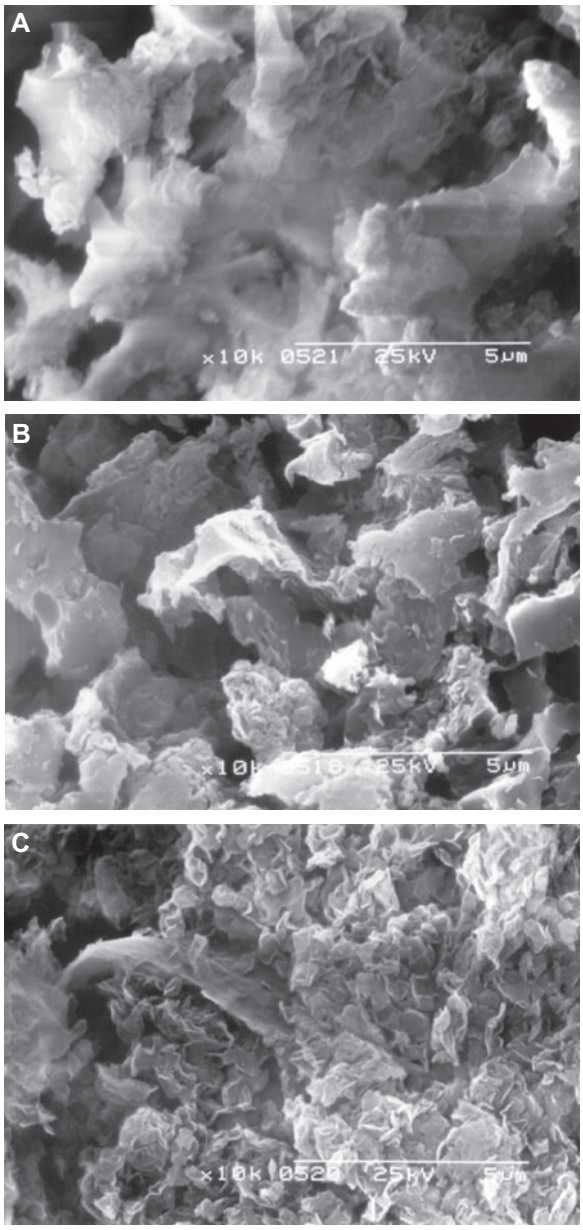

Figure 15 SEM micrographs of typical remaining crud solids following the demulsification by S-PHP-Na. Scale bar=5 μm. Washed by: (A) water; (B) ethanol; and (C) dichloromethane followed by hexane.

when they are compared with the EDAX spectrum shown in Figure 16A. Figure 19B shows markedly low Pd and P peaks, but a pronounced sodium peak, indicating that it is mainly an organic material. The EDAX spectrum of the total area of the micrograph in Figure 18A (i.e., Figure 19A) shows the presence of a large quantity of Pd, whereas the spectrum of the bright area in the same micrograph (i.e., Figure 19B) indicates very little Pd. The spectrum of the dark region of the micrograph also showed a large quantity of palladium, but lesser sodium, than that of the total area. This, and the bright white color, may indicate that the crud was not only formed from Pd complexes of the degradation products, but contained other components. Therefore, the solids in IFC may be in fact two types differentiated by the presence of the organics.

3.3.2. Effect of the particle size of PHP The effect of the particle size of the S-PHP-Na on the demulsification was investigated for M_{PHP}/V_T=2.34 mg/l. The results are shown in Table 3. It appears that the larger particles performed slightly better than smaller particles. The amount of the sediments in the aqueous phase seemed to be the same size for all the PHP particle fractions being investigated and they had the same appearance. The total amount of sediments, and the amount of the suspended sediments, got smaller with decreasing particle size. This observation indicated that the sediments might have not been only the PHP particles, but rather a mixture of the PHP particles with solid products of the demulsification. This was checked by mixing the same amount of PHP particles as above with a mixture of the aqueous (15 ml) and organic phase (15 ml) only. It was observed that as soon as the PHP particles came into contact with the liquid in the tube, they started crumbling into much smaller particles, as a result of differential swelling which induces internal stresses. These PHP particles and those sedimented after the demulsification, had the same appearance, showing that the sediments were PHP particles.

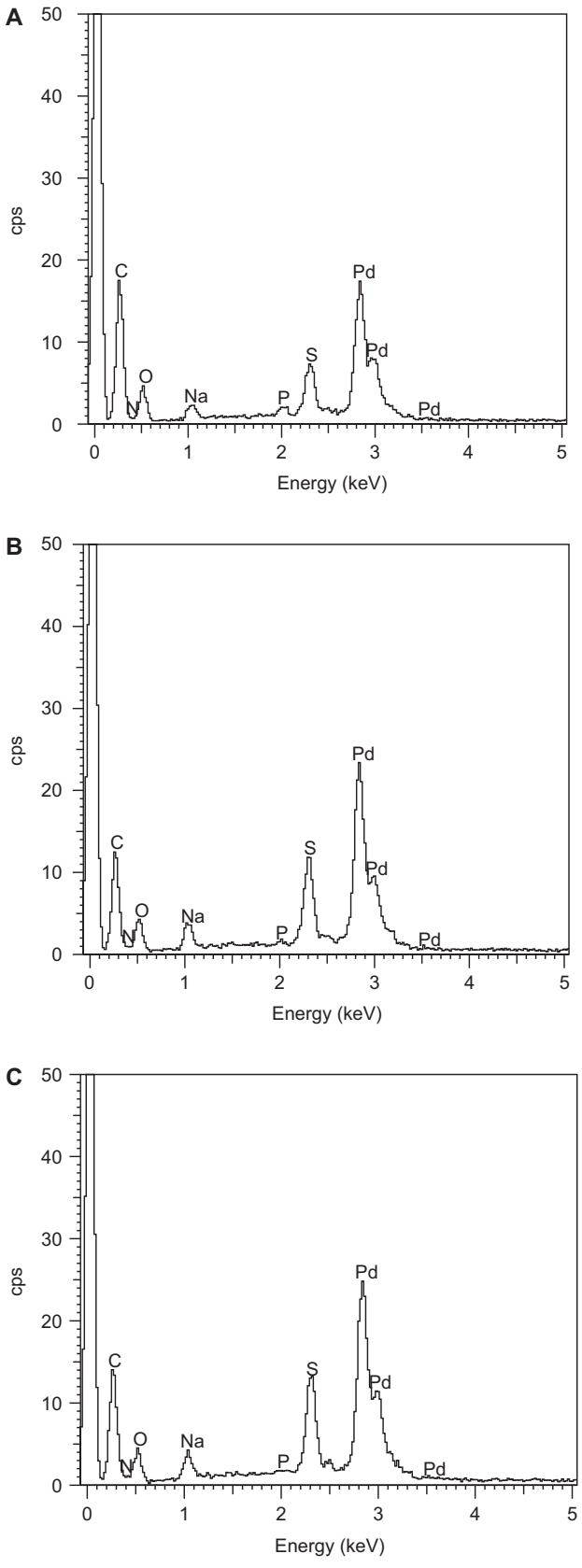

Figure 16 EDAX spectra of typical remaining crud solids following the demulsification by S-PHP-Na. Washed by: (A) water; (B) ethanol; and (C) dichloromethane followed by hexane.

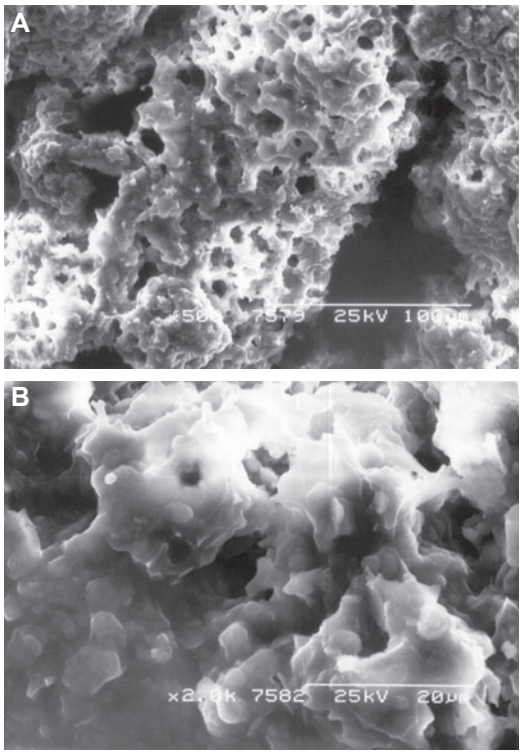

Figure 17 SEM micrographs of the hydrophilic PHP particles remaining in the crud phase after demulsification of the remaining crud from the first demulsification. Magnification: (A) scale bar=100 μm, (B) scale bar=20 μm.

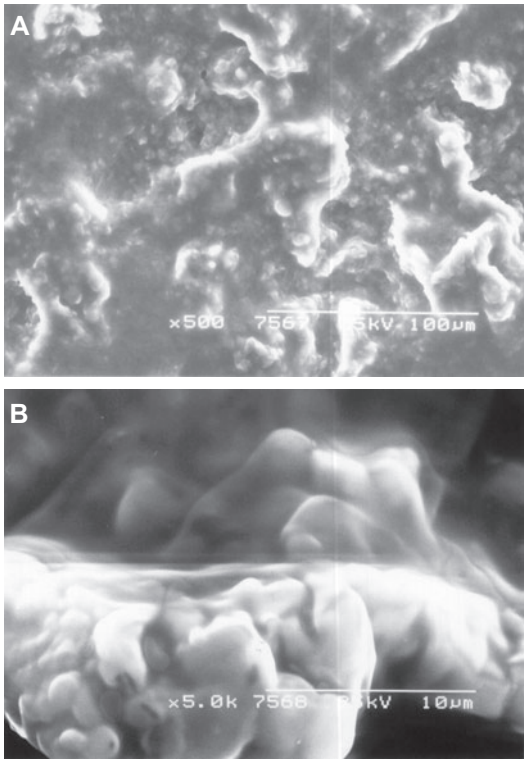

Figure 18 SEM micrographs of fine crud particles. Magnification: (A) scale bar=100 μm, (B) scale bar=10 μm.

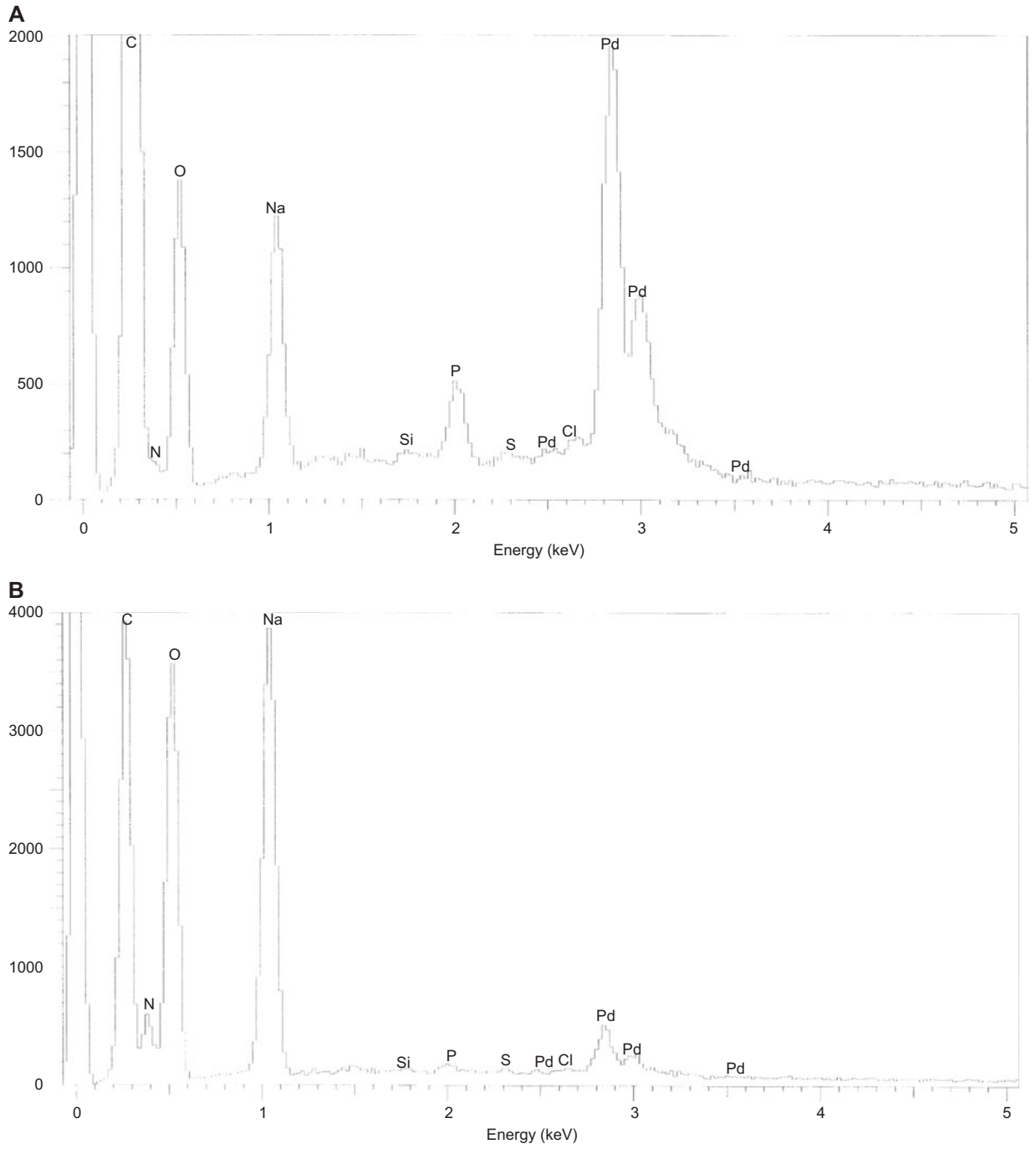

Figure 19 (A) EDAX spectrum of fine crud particles (total area shown in Figure 18A); (B) EDAX spectrum of fine crud particles (bright area of in Figure 18A shown in Figure 18B).

In contrast to the sediments after the demulsification, the smaller particles here were positioned at the top of the aqueous phase. The reason for the particle sedimentation following the demulsification, is that PHP particles become heavier as they bind the crud solids in their cellular structure.

3.3.3. Effect of the degree of sulfonation of PHP The degree of the sulfonation of the PHP represents its hydrophilic characteristics. The effect of the degree of the sulfonation on the demulsification was investigated with S-PHP-Na particles of -1000+250 μm size, for varying types of IFC, and the ratio of M_{PHP}/V_T (in g/l). For a typical IFC (produced at 60°C with [Pd] = 1 g/l and $NaNO_2$ addition rate of 10 g/l), the results are shown in Table 4. It appears that the degree of the sulfonation was important in the demulsification and that demulsification performance increased with increasing the degree of sulfonation up to a certain point, beyond which, the demulsification capacity remained unchanged with increasing the degree of the sulfonation. This data is shown in graph form in Figure 20 (triangular symbol). Some more

Table 3 The effect of the particle size on the demulsification. M_{PHP}/V_T = 2.34 mg/ml, room conditions.

Test no	Particle size (μm)	$[V_C]_i$ (ml)	$[V_C]_l$ (ml)	$[V_{aq}]_i$ (ml)	$[V_{aq}]_l$ (ml)	$[V_{or}]_i$ (ml)	$[V_{or}]_l$ (ml)	D (ml/g)
1	+1000	24	13	0.0	14	6	3	200
2	-1000+710	23	13	0.0	13	7	4	186
3	-710+500	23	13	0.0	13	7	4	186
4	-500+250	23	13	0.0	13	7	4	186
5	-250	23	13	0.0	12	7	5	171

Table 4 The effect of the degree of the sulphonation (acid form) on the demulsification. M_{PHP}/V_T = 3 mg/ml, room conditions.

Test no	Degree of sulphonation (%)	$[V_C]_i$ (ml)	$[V_C]_l$ (ml)	$[V_{aq}]_i$ (ml)	$[V_{aq}]_l$ (ml)	$[V_{or}]_i$ (ml)	$[V_{or}]_l$ (ml)	D (ml/g)
1	0	24	26	0	0	6	5	0
2	10	23	19	0	5	7	7	125
3	20	23	14	0	16	7	1	400
4	40	22	6	0	16	8	8	533
5	92	23	6	0	16	7	8	533
6	92	23	6	0	16	7	8	533
7	92	23	6	0	16	7	8	533

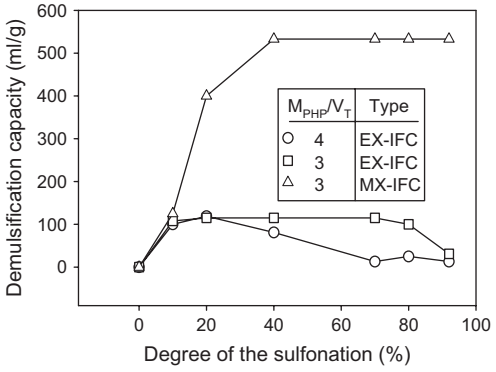

Figure 20 Effect of the degree of the sulphonation for varying type of crud and the ratio of mass of PHP to the total volume of initial tube content (M_{PHP}/V_T). IFC production conditions: [Pd]=1 g/l; $NaNO_2$ addition rate=10 g/l. Reaction temperature T=60°C (EX-IFC) and T=80°C (MX-IFC).

tests on the effect of the sulfonation degree were performed for a different type of IFC and varying M_{PHP}/V_T. The results are given in Tables 5 and 6, as well as shown in Figure 20. It seems that the demulsification capacity of S-PHP, with a given degree of sulfonation, varied depending on the type of IFC. As the degree of the sulfonation becomes greater, PHP becomes more hydrophilic in character and it holds more volumes of the aqueous phase in its cellular structure. Thus, in effect, a lesser amount of free aqueous phase separates and the separation capacity is decreased with increasing ratio of M_{PHP}/V_T (see Eq. 1).

3.3.4. Effect of the neutralization of PHP The effect of neutralization of the S-PHP on the demulsification, was investigated for different degrees of sulfonation with S-PHP-Na particles of -1000+250 μm size and $M_{S\text{-}PHP\text{-}Na}/V_T$=3 mg/l. The results are shown in Table 7. The effect of the neutralization can be evaluated by comparing the values of the demulsification capacity (D) in this table, with that of S-PHP in Table 4. A careful inspection of these tables indicates that neutralization did not significantly influence the demulsification performance of the S-PHP.

3.3.5. Effect of the contact time and the type of IFC The effect of the time passed from the first mixing and the subsequent mixings during this time period (the contact time),were investigated for varying S-PHP-Na mass (M_{PHP}).

Table 5 The effect of the degree of the sulphonation on the demulsification. M_{PHP}/V_T =3 mg/ml, room conditions.

Test no	Degree of sulphonation (%)	$[V_C]_i$ (ml)	$[V_C]_l$ (ml)	$[V_{aq}]_i$ (ml)	$[V_{aq}]_l$ (ml)	$[V_{or}]_i$ (ml)	$[V_{or}]_l$ (ml)	D (ml/g)
1	0	17	18	0	0	3	2	0
2	10	17	10	0	7	3	3	108
3	20	17	8	0	7.5	3	4.5	115
4	40	17	11.5	0	7.5	3	2	115
5	70	17	10	0	7.5	3	3	115
6	80	17	10	0	6.5	3	3.5	100
7	92	17	14	0	2.0	3	4	31

Table 6 The effect of the degree of the sulphonation on the demulsification. M_{PHP}/V_T =4 mg/ml, room conditions.

Test no	Degree of sulphonation (%)	$[V_C]_i$ (ml)	$[V_C]_l$ (ml)	$[V_{aq}]_i$ (ml)	$[V_{aq}]_l$ (ml)	$[V_{or}]_i$ (ml)	$[V_{or}]_l$ (ml)	D (ml/g)
1	0	17	18	0	0	3	2	0
2	10	17	10	0	8	3	2	100
3	20	17	9	0	9.5	3	1.5	119
4	40	17	10.5	0	6.5	3	3.5	81
5	70	17	17	0	1	3	2	13
6	80	17	16	0	2	3	2	25
7	92	17	16	0	1	3	3	13

Table 7 The effect of the neutralisation of the sulphonated PHP on the demulsification. M_{PHP}/V_T = 3 mg/ml, room conditions.

Test no	Degree of sulphonation (%)	$[V_C]_i$ (ml)	$[V_C]_l$ (ml)	$[V_{aq}]_i$ (ml)	$[V_{aq}]_l$ (ml)	$[V_{or}]_i$ (ml)	$[V_{or}]_l$ (ml)	D (ml/g)
1	0	24	26	0	0	6	5	0
2	10	22	17	0	5	8	8	125
3	20	22	12	0	15	8	3	375
4	40	22	6	0	16	8	8	533

The results are shown in Figure 21. At first, for M_{PHP}=0.03 g, no separation occurred, but as the time passed, it yielded the highest separation among all. For $0.1 \geq M_{PHP} > 0.03$, the volume of the initially separated aqueous phase did not change significantly with M_{PHP}. This means that the separation capacity is higher for the smaller M_{PHP} due to the virtue of its definition (see Eq. 1).

After 25 days, subsequent shakings did not cause any significant changes in the volumes of the separated aqueous phase for each mass of PHP. The demulsification performance of S-PHP-Na was dependent on the type of the IFC (Figure 20), as in the case of non-sulfonated PHP, but also depending on the time passed following the first mixing (Figure 21). It appeared that if a fast separation is required, then a smaller amount of S-PHP-Na with a high degree of sulfonation (40–80%) is needed. However, if the separation time is not a concern, better separation performances can be achieved by allowing the mixture of S-PHP-Na with a smaller degree of sulfonation and IFC to rest for longer periods.

3.3.6. Mixture of hydrophilic and hydrophobic PHPs The effect of a mixture of the hydrophilic and hydrophobic PHPs on the demulsification capacity was investigated for a fixed mass of S-PHP-Na (0.06 g), with a varying mass of hydrophobic PHP (0 to 1.06 g). The results are shown in Figure 22. For the first week, the addition of hydrophobic PHP slightly decreased the separation performance. However, as the time passed further, for 1.06 g hydrophobic PHP addition, the separation was reduced dramatically (93%) with respect to its first day separation, as well as to the case of no hydrophobic PHP addition. A slight improvement (11%) in the separation was observed for 0.3 g hydrophobic PHP addition in the third week, with respect to the case of no hydrophobic PHP addition. The results indicate that in batch mode demulsification, a mixture of the rigid

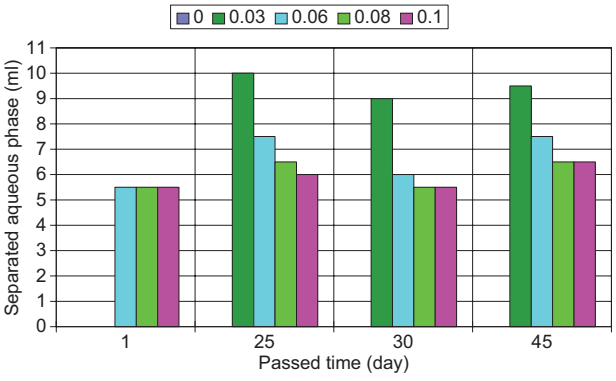

Figure 21 Effect of S-PHP-Na mass on the aqueous phase separation as a function of time. Legend shows the mass of PHP in g.

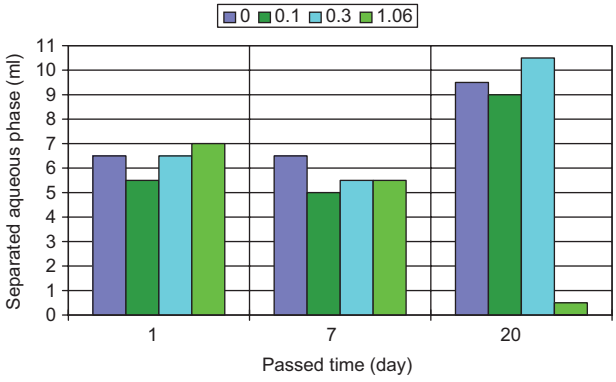

Figure 22 Effect of the mixture of S-PHP-Na and PHP as function of time on the demulsification of crud. S-PHP-Na=0.06 g; mass of PHP is given in the legend in g.

hydrophilic and the rigid hydrophobic PHP does not cause any significant improvement in the separation performance, but may yield a dramatic reduction if the mass of the rigid hydrophobic PHP is above a certain limit.

4. Conclusions

IFC simulants were made for varying Pd concentrations, reaction temperatures and amounts of daily sodium nitrite ($NaNO_2$) addition. The level of the degradation was inferred from the volumes of IFCs produced, as well as by quantitative measurements of -COOH, DBP, TOC, and Pd concentrations in the samples collected from the aqueous and the solvent phases (no [TOC] measurement in the solvent phase) as a function of the time. The results indicated that the impact order in the production of IFC was: temperature, Pd concentration and daily $NaNO_2$ addition.

Hydrophilic PHP samples, with varying degrees of sulfonation, were prepared and used in demulsification tests. The degree of the sulfonation was a function of PHP particle size and reaction time and temperature. A desired degree of the sulfonation could be obtained by different combinations of these governing parameters.

The results obtained from the batch mode demulsification tests indicated that it is possible to partially demulsify the IFC in batch mode, by contacting them with the PHP. Among all the different types, the hydrophilic (sulfonated) PHP was found to be the most effective. Since the main effect of the sulfonation is to give a certain degree of hydrophilicity to the PHPs, we can assume that the degree of hydrophilicity of PHP is an important factor in achieving high demulsification capacity. However, although hydrophilicity of PHP is important in adsorbing the mobile aqueous phase and hence the adsorption of surface active species, its demulsification characteristics may be due to the "surfactant like" structure of the sulfonated PHP walls, with hydrophobic and hydrophilic sites, which allow the formation of stable surfactant structures within the pores [5]. The neutralization of the sulfonated PHP did not significantly alter its demulsification characteristics. It was observed that the larger PHP particles had a slightly better demulsification performance than smaller particles.

Limited numbers of continuous mode demulsification tests using rigid hydrophobic PHP, showed that it was possible to break down IFC in a continuous mode. The results indicated that about 85% of the aqueous phase in IFC could be separated. However, the solvent phase, as well as the solids, was absorbed by the PHP. These results suggest that PHP might well prevent the formation of IFC if the solution is circulated through a S-PHP medium during the IFC simulant making tests. Therefore, sulfonated PHP can be used to remove surface active species from liquids by, for example, cross-flow filtration mode and subsequently recover them in a concentrated form.

The demulsification by PHP indicates that PHP selectively absorbs the surface active species instead of absorbing all of the available aqueous phase. However, there appears to be some IFC left over (residual IFC) at the solvent/aqueous phase interface which cannot be removed by the addition of extra PHP. This may be due to presence of two or more types of emulsion with different stabilization mechanisms.

The use of sulfonated PHP in the continuous demulsification of water-in-crude oil emulsion, with or without an applied electric field, yielded very similar results [3, 7, 12]. The so called "confinement phenomenon" [5, 26] was proposed for the demulsification of water-in-oil emulsions, as well as for the removal of surfactants from water through the formation of secondary membrane during cross-flow microfiltration. Similarly, sulfonated PHPs were also used to remove surface active species (tars) from syngas generated during the gasification of biomass [33–35]. The underlying mechanism appears to be the same, whereby surface active species have lower free energy within microscopic pores, wherein they form stable structures [26].

The formation of IFC is also present in other solvent extraction processes, such as those encountered in hydrometallurgy in which IFC often inhibits the recycling of the extractant and increases its loss [36].

Acknowledgements

This research and Dr Pekdemir were fully supported by British Nuclear Fuels Ltd (BNFL) under contract No: A808096. Dr John Vickers was seconded by BNFL to carry out the research at Newcastle University for 3 years. We are grateful for their support and permission to publish.

References

[1] Ekott EJ, Akpabio EJ. *J. Eng. Appl. Sci.* 2010, 5, 447–452.
[2] Nour AH, Yunus RM, Nour AH. *World Academy Sci. Eng. Technol.* 2010, 62, 188–193.
[3] Akay G, Vickers J. Methods for separating oil and water, US Patent 7780854, 2010.
[4] Colle RD, Longo E, Fontes SR. *J Membrane Sci.* 2007, 28, 58–66.
[5] Akay G. Bioprocess and chemical process intensification. In *Encyclopedia of Chemical Processing*, Lee, S, Eds., Marcel Dekker: New York, 2006, 183–199.
[6] Stark JL, Asomaning S. *Energy Fuel* 2005, 19, 1342–1345.
[7] Pekdemir T, Akay G, Dogru M, Merrells RE, Schleicher B. *Sep. Sci. Technol*. 2003, 38, 1161–1183.
[8] Eow JS, Ghadiri M. *Colloids Surf A* 2003, 219, 253–279.
[9] Eow JS, Ghadiri M, Sharif A, Williams T. *Chem. Eng. J*. 2001, 84, 173–192.
[10] Tirmizi NP, Raghuraman B, Wiencek J. *AIChE J.* 1996, 42, 1263–1276.
[11] Taylor SE. *Chem. Eng. Res. Des.* 1996, 74, 526–540.
[12] Akay G, Noor ZZ, Dogru M. Process intensification in water-in-crude oil emulsion separation by simultaneous application of electric field and novel demulsifier adsorbers based on Polyhipe Polymers. In *Microreactor Technology and Process Intensification*, Wang, Y, Holladay, J, Eds., Oxford University Press: Oxford, 2005, Ch. 21.
[13] Marshall W. *Nuclear Power Technology*, Vols. 1 and 2, Oxford University Press: Oxford, UK, 1983.
[14] Ritcey GM, Wong EW. *Hydrometallurgy* 1985, 15, 55–61.
[15] Healy TV, McKay HAC. *RECUEIL.* 1956, 75, 730–736.

[16] Rochon AM, Nowak ZP, Zagorski ZP. *Radiochem. Radioanal. Letters* 1976, 27, 1–8.
[17] Adamov VM, Andreev VI, Belyaev BN, Markov GS, Polyakov MS, Ritari AE, Shilnikov AY. *Kerntechnik* 1990, 55, 133–137.
[18] Smith DN, Edwards HGM, Hughes MA, Courtney B. *Sep. Sci. Technol*. 1997, 32, 2821–2849.
[19] Shuyao Y, Yu S, Tianzhen T. *Radiat. Phys. Chem*. 1989, 33, 599–602.
[20] Sugai H, Munataka K. *Nuclear Technology* 1992, 99, 235–241.
[21] Hardy CJ, Scargill D. *J. Inorg. Nucl. Chem.* 1961, 17, 337–349.
[22] Akay G, Wakeman RJ. *J. Memb. Sci*. 1994, 88, 177–195.
[23] Akay G, Wakeman RJ. *Chem. Eng. Sci*. 1994, 49, 271–283.
[24] Akay G, Bhumgara Z, Wakeman RJ. *Chem. Eng. Res. Design* 1995, 73, 783–796.
[25] Akay G, Wakeman RJ. *Chem. Eng. Research Design* 1996, 74, 517–525.
[26] Akay G. Confinement phenomenon and its application to membrane demulsification and separation of water/oil/colloidal solid emulsions. British Nuclear Fuels Ltd (BNFL) Report, Nottingham University, Nottingham; UK, 1996.
[27] Akay G, Odirile PT, Keskinler B, Wakeman RJ. Crossflow microfiltration characteristics of surfactants, In *Surfactant-Based Separations,* Scamehorn, I.F., Harwell, J.H., Eds., ACS Symposium Series 1000, 740, 175.
[28] Akay G, Birch MA, Bokhari MA. *Biomaterials* 2004, 25, 3991–4000.
[29] Akay G, Bokhari MA, Byron VJ, Dogru M. Development of nano-structured materials and their application in bioprocess-chemical process intensification and tissue engineering. In *Chemical Engineering Trends and Developments*, Galan, MA, Del Valle, EM, Eds., Ch. 7, 171, Wiley: London, UK, 2005.
[30] Akay G, Erhan E, Keskinler B. *Bioeng. Biotechnol.* 2005, 90, 180–190.
[31] Akay G, Noor ZZ, Calkan OF, Ndlovu TM, Burke DR. Process for preparing a functionalised PolyHIPE polymer, US Patent 07820729, 2010.
[32] Wakeman RJ, Bhumgara Z, Akay G. *Chem. Eng. J.* 1998, 70, 133–141.
[33] Dogru M, Akay G. Catalytic gasification, Japanese Patent, 4781274, 2011.
[34] Akay G, Jordan CA. *Energy Fuels* 2011, 25, 2274–2283.
[35] Jordan CA, Akay G. *Fuel* 2012, 91, 253–263.
[36] Ning P, Cao H, Liu C, Li Y, Zhang Y. *Hydrometallurgy* 2009, 97, 131–136.

Received October 28, 2011; accepted December 8, 2011